Proceedings World Geothermal Congress 2026, Calgary, Canada, June 8—11, 2026

WGC 2026
FORGING GEOTHERMAL INNOVATION
JUNE 8 - 11, 2026 | CALGARY, CANADA

Corrosion of Type 430 Stainless Steel at 250 °C in Acidic Fluids

N. Hirabayashi*[1], M. Morita[2]
Department of Marine Engineering, Tokyo University of Marine Science and Technology, Japan[1]
Faculty of Marine Science and Technology, Tokyo University of Marine Science and Technology[2]
*Email：m254010@edu.kaiyodai.ac.jp

国立大学法人 東京海洋大学
Tokyo University of Marine Science and Technology

INTRODUCTION

- About 30% of geothermal wells in Japan produce acidic fluids. However, their utilization has been limited because materials with high corrosion resistance are considered expensive. If lower-cost materials can be applied, acidic geothermal brine could be more effectively utilized. Therefore, reliable corrosion data are required. In Japan, some acidic geothermal fluids contain large amounts of chloride ions.
- One of an acidic geothermal fluids are believed to contain large amounts of chloride ions in Japan.
- Type 430 stainless steel is a conventional and readily available material with moderate corrosion resistance.
- In this study, corrosion tests of Type 430 stainless steel were conducted in acidic chloride fluids under subcritical conditions (250 °C). The corrosion mechanism was considered.

METHODS

Corrosion test were conducted to evaluate the corrosion behavior of ferritic stainless steel in acidic geothermal environments.

Test solution: simulated acidic geothermal water (pH 3.5, NaCl 30,000 ppm, dissolved oxygen ≤ 0.1 mg/L)

Specimens: ferritic stainless steel (Type 430) under two conditions: cold-rolled (strained) and solution-annealed (strain-free).

Test conditions: 72 h continuous flow corrosion test at 250 °C and 30 MPa.

Analyses: SEM observation, XPS analysis (wide scan and depth profiling), and AES elemental mapping.

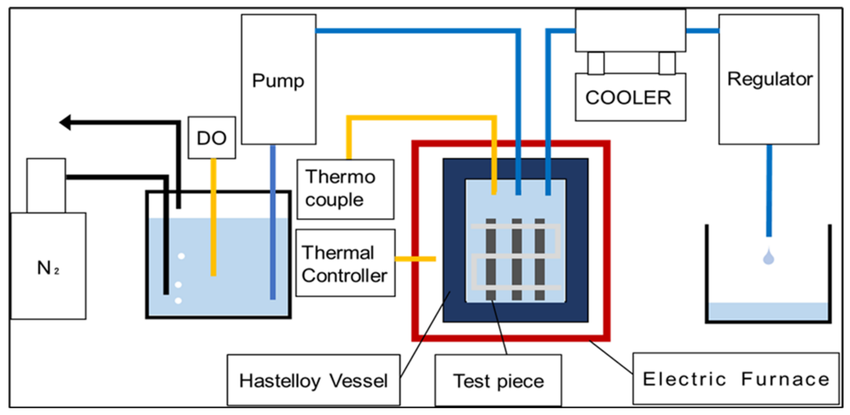


Fig. 1. Schematic diagram of the corrosion test apparatus used in this study.

RESULTS

(1) Corrosion Rate

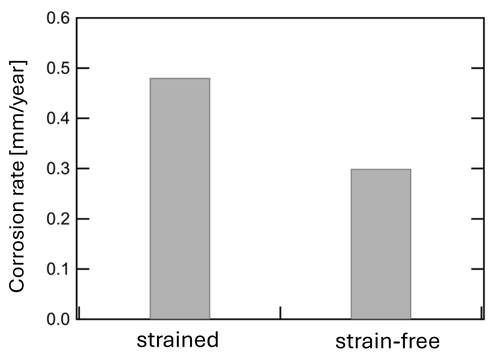


Fig. 2. Corrosion rate of strained and strain-free specimens.

The corrosion rate of the strained specimen was approximately 0.5 mm/year, whereas that of the strain-free specimen was about 0.3 mm/year (Fig. 2).

(2) Surface Observation (Optical Microscopy)

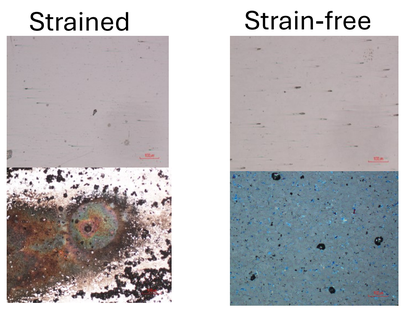


Fig. 3. Optical micrographs of strained and strain-free specimens before (top) and after (bottom) the flow test.

Pitting corrosion was evident on the specimen after the flow test (Fig.3), whereas the strain–free specimen showed only incipient pits.

(3) Surface Observation (SEM)

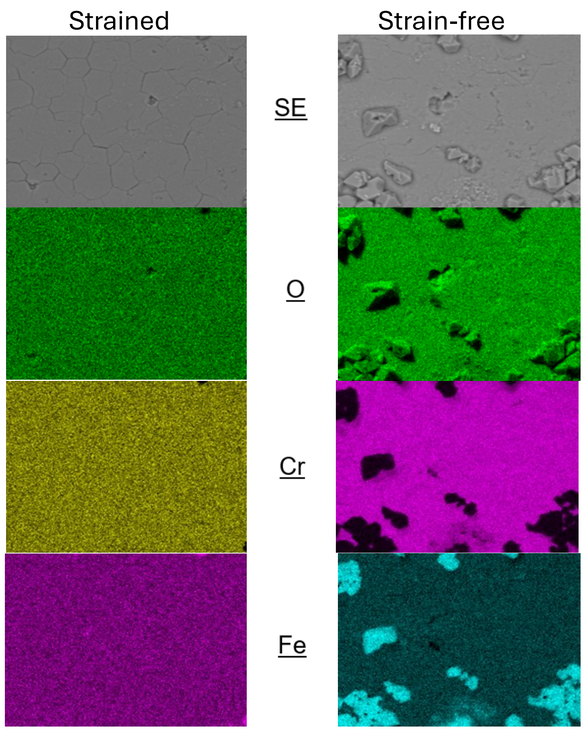


Fig. 4. SEM surface micrographs and elemental maps of strained and strain-free specimens after the 250 °C flow test.

Strained: The strained specimen showed a relatively smooth surface with clear grain boundaries. The surface was dominated by Fe, and Cr was not clearly detected at the outermost surface.

Strain-free: The strain-free specimen showed oxide particles and surface cracks. Cr-enriched areas were locally observed, suggesting the formation of more protective oxide patches.

(4) XPS Wide Scans

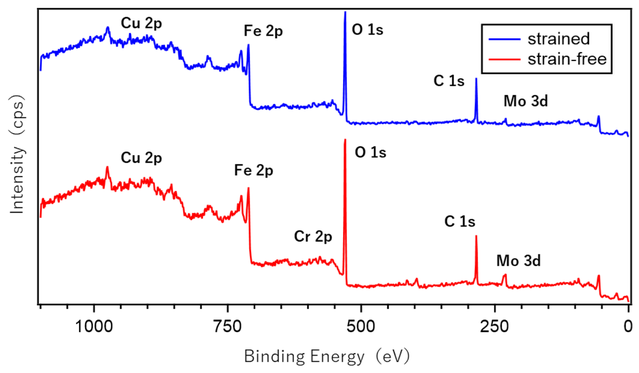


Fig. 5. XPS wide-scan spectra of strained and strain-free specimens after flow test.

Strained: Cu, Fe, O, C, and Mo peaks were detected.

Strain-free: Cu, Fe, Cr, O, C, and Mo peaks were detected.

The presence of Cr peaks in the strain-free specimen suggests the formation of Cr-containing oxide layers.

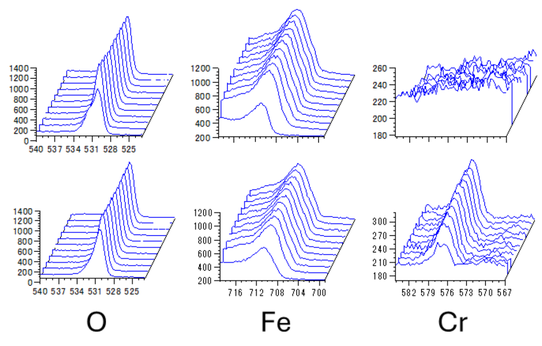


Fig. 6. XPS depth profiles (O, Fe, Cr): strained (top), strain-free (bottom).

Strained: Fe and O signals were mainly observed, with no clear Cr enrichment through the depth.

Strain-free: Distinct Cr enrichment was observed near the metal/oxide interface.

This Cr enrichment suggests the formation of a protective Cr-rich oxide layer.

(5) AES Element Maps

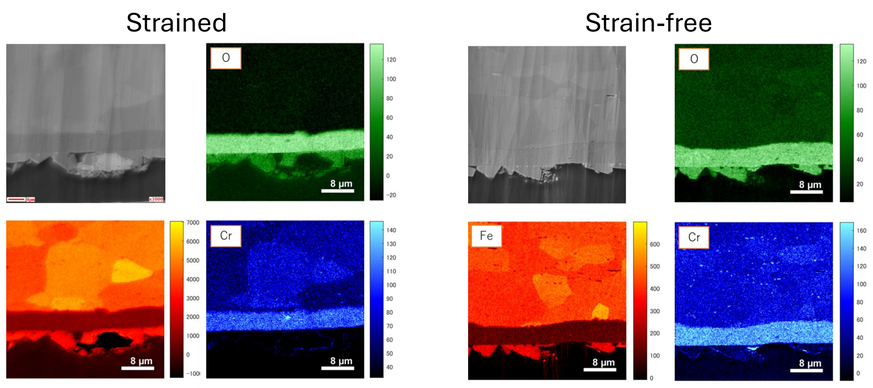


Fig. 7. AES elemental maps showing the oxide-layer structure of strained and strain-free specimens.

Strained

- A continuous oxide layer was observed, partially covered by discontinuous granular oxides.
- The continuous layer consists of Fe–Cr mixed oxides, while the outer layer is Fe–rich.
- A possible Cr–depleted region was observed beneath the oxide/metal interface.

Strain-free

- Discontinuous granular oxides are formed on the continuous oxide layer.
- The continuous layer is mainly composed of Cr oxides.
- The outer layer consists mainly of Fe oxide.

These results indicate that Cr-rich oxides are preferentially formed in the strain-free specimen, which likely contributes to improved corrosion resistance.

DISCUSSION

The strained specimen likely contained a high density of dislocations introduced by cold working, which enhanced Fe diffusion during oxidation.

As a result, a thicker Fe-rich oxide layer was formed on the surface.

Preferential oxidation of Fe may have caused local Cr depletion near the metal/oxide interface, leading to a less protective oxide layer (Fig. 8).

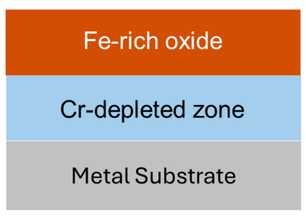


Fig. 8. Oxide layer growth model (strained)

CONCLUSION

- Strain-free specimens exhibited lower corrosion rates than strained specimens.
- In strained Type 430 specimens, pitting corrosion associated with the growth of Fe-rich oxides was observed.
- These results suggest that strain-free Type 430 stainless steel can provide improved corrosion resistance in acidic geothermal environments.

Acknowledgements

This research was supported by Moritani Ikueikai Foundation. The authors gratefully acknowledge Prof. Toshiaki Masuda (Shizuoka University) for providing facilities and support, and MEXT Materials Open Platform Project (JPMXP1225HK0081) at Hokkaido University, with special thanks to Mr. Keita Suzuki for TEM assistance

REFERENCES

The Japan Society of Corrosion Engineering (Ed.): High Temperature Oxidation and Corrosion of Metallic Materials (in Japanese), Maruzen, 1982.

H. Fujikawa, J. Murayama, and N. Fujino: High Temperature Oxidation Behavior of Chromium Ferritic Stainless Steels, *Tetsu-to-Hagane*, **69 (6)**, (1983), 678-685.